Iron Transformation and Ash Fusibility during Coal Combustion in Air and O2/CO2 Medium

ARTICLE *in* ENERGY & FUELS · FEBRUARY 2012

Impact Factor: 2.79 · DOI: 10.1021/ef201786v

6 AUTHORS, INCLUDING:

Dunxi Yu
Huazhong University of Science and Technology
40 PUBLICATIONS **404** CITATIONS
SEE PROFILE

Hong Yao
Huazhong University of Science and Technology
165 PUBLICATIONS **1,193** CITATIONS
SEE PROFILE

energy&fuels

Article

pubs.acs.org/EF

Iron Transformation and Ash Fusibility during Coal Combustion in Air and O_2/CO_2 Medium

Dunxi Yu,* Liang Zhao, Zuoyong Zhang, Chang Wen, Minghou Xu, and Hong Yao

State Key Laboratory of Coal Combustion, Huazhong University of Science and Technology, 1037 Luoyu Road, Wuhan 430074, People's Republic of China

ABSTRACT: Little work has been performed on the transformation of iron and ash fusibility during oxy-coal combustion, which is of great significance to assessing ash deposition propensity. A high-iron bituminous coal was burnt at 1300 °C in a laboratory drop-tube furnace under four conditions: (1) 21 vol % O_2/79 vol % N_2 (air-firing), (2) 21 vol % O_2/79 vol % CO_2 (oxy-firing), (3) 27 vol % O_2/73 vol % CO_2 (oxy-firing), and (4) 32 vol % O_2/68 vol % CO_2 (oxy-firing). The bulk ash samples were subjected to X-ray fluorescence and Mössbauer spectroscopic analyses. The effects of changing from air combustion to O_2/CO_2 combustion and the effects of varying the O_2 level in O_2/CO_2 combustion on iron transformation and ash fusibility were investigated. The results show that varying the combustion condition has insignificant effects on the elemental composition of coal ashes but has appreciable effects on the relative proportions of iron combustion products that were identified as hematite, magnetite, and Fe−glass phases. This indicates that speciation analysis is as important as bulk analysis for thorough ash characterization. Replacing N_2 in air with CO_2 results in a higher content of hematite but a lower content of magnetite. Increasing the O_2 level in O_2/CO_2 combustion increases the formation of hematite but decreases the formation of magnetite. In contrast, the amount of Fe−glass phases remains almost unchanged. An appreciable fraction (about 8% Fe) of hematite/magnetite seems to crystallize out of the molten glass phases during combustion, and it is not significantly affected by changing combustion conditions. The fusion temperatures of the oxy-fired ashes are higher than those of the air-fired ash and increase with the inlet O_2 level. A positive correlation between the hematite content and the ash fusion temperatures is observed.

1. INTRODUCTION

Oxy-fuel combustion (O_2/CO_2 combustion) is a promising option for capturing CO_2 from coal-fired power plants.[1] The successful design and operation of oxy-fired pulverized coal boilers require comprehensive knowledge of ash deposition characteristics, which have a major impact on the safety and economic performance of the boilers. Iron has been identified as an important element contributing to ash deposition,[2] and its transformation behavior must be well-addressed for the assessment of ash deposition tendency under oxy-firing conditions.

There has been a substantial body of literature available on the fate of iron under air-firing conditions. Iron in coal is usually present as pyrite (FeS_2) and can also be in the form of siderite ($FeCO_3$), ankerite [$CaFe(CO_3)_2$], and clay minerals (e.g., Fe−illite), depending upon the coal type.[3,4] The evolution of pyrite in an oxygen-containing atmosphere is a complicated process and may proceed by different mechanisms under different conditions.[5] Generally, at lower temperatures (<about 800 K) and higher oxygen concentrations, pyrite will be directly oxidized to iron oxides [mainly magnetite (Fe_3O_4) and/or hematite (α-Fe_2O_3)]. In contrast, at higher temperatures (>about 800 K) and lower oxygen concentrations, pyrite will evolve through a two-step process: the thermal decomposition of the pyrite to form porous pyrrhotite ($Fe_{1-x}S$), which is followed by pyrrhotite oxidation. Parameters such as temperature, particle size, flow condition, residence time, and properties of the surrounding atmosphere can all affect the final products of pyrite transformation. For example, it can be easily oxidized to iron oxides in an oxidizing environment, while pyrrhotite is one of the major products of pyrite decomposition in a non-oxidizing environment. In comparison to pyrite, iron carbonates, such as siderite and ankerite, are subjected to relatively simple processes. They are unstable and decompose at typical flame temperatures into the corresponding oxides and carbon dioxide gas.[6] Iron in clay minerals is a fluxing agent and will mostly remain in the matrix after combustion. However, the final oxidation states of iron are dependent upon the local temperature and atmosphere.[4] Iron-bearing minerals can be included and excluded. Their associations with the carbon matrix are also important in determining the fate of iron during coal combustion. Unlike the excluded iron minerals, the included iron minerals undergo higher combustion temperatures and more reducing atmospheres because of carbon oxidation. In addition, the included iron has opportunities to become in contact with other minerals (e.g., clay minerals) in the same coal particle. Therefore, interactions between these minerals may occur and further increase the complexity of iron transformation.[7]

In comparison to air−coal combustion, oxy-coal combustion leads to changes in a number of parameters and, therefore, may have significant effects on iron transformation. These changes are mainly due to differences in gas properties between CO_2 and N_2.[1,8] For example, CO_2 has a higher heat capacity than N_2, which affects the particle combustion temperature. With an

Special Issue: 7th International Symposium on Coal Combustion

Received: November 15, 2011
Revised: December 23, 2011
Published: December 26, 2011

   dx.doi.org/10.1021/ef201786v | Energy Fuels 2012, 26, 3150−3155

Table 1. Fuel Analysis Data

proximate analysis (wt %, ad)				ultimate analysis (wt %, ad)				
moisture	ash	volatile matter	fixed carbon	C	H	N	S	O (by difference)
9.65	7.99	36.78	45.58	64.67	5.59	1.12	3.98	7
ash composition (wt %)								
Na_2O	MgO	Al_2O_3	SiO_2	P_2O_5	SO_3	K_2O	CaO	TiO_2	Fe_2O_3
1.51	0.98	17.66	49.28	0.11	2.22	2.26	1.87	0.85	14.57

increasing CO_2 in the bulk gas, a greater CO/CO_2 ratio was predicted,[9] indicating a more reducing environment inside the char particle. In addition, CO_2 was also reported to be heavily involved in combustion reactions.[10] The effects of these changes on iron transformation have been less investigated. Only limited data are available in the literature. Bhargava et al. conducted an *in situ* high-temperature X-ray diffraction study of pyrite decomposition in pure CO_2.[11] They found that heating the sample at 800 °C and above led to the formation of magnetite and hematite. This was attributed to the dissociation of CO_2 into CO and O_2 that favored the formation of iron oxides. Fegley et al. showed the dissociation of CO_2 into CO and O_2 at 500 °C and observed the formation of hematite and maghemite (γ-Fe_2O_3) in $CO-CO_2$ gas mixtures.[12] The transformations of included and excluded iron in Chinese coals were investigated by Sheng's group.[13,14] In one study, it was found that, in comparison to O_2/N_2 combustion, O_2/CO_2 combustion at the same oxygen concentration led to more iron melting into glass silicates and less iron oxides.[13] The reason was that the lower char combustion temperature and the high CO concentration within the particles slowed the transformations of included pyrite and siderite to oxides while favored their transformations to iron glass. In another study, it was concluded that the transformation of excluded pyrite was not significantly affected by replacing N_2 with CO_2 during pulverized coal combustion.[14] Our recent data on the Illinois No. 6 coal showed that the iron content in the oxy-fired deposits collected on the deposition coupon in the high-temperature combustion zone was apparently lower than that in the air-fired deposit, although the contents of iron were similar in the bulk ashes isokinetically collected on filters at lower temperatures.[15] It indicated differences in the transformation of iron and its deposition behavior between air- and oxy-firing. In summary, comparative data are still lacking as to iron transformation under oxy-firing conditions. In addition, the effects of oxy-firing on ash fusibility, an important indicator of the slagging propensity, have not been clarified.

The present work aims to provide experimental data on how oxy-coal combustion affects iron transformation and ash fusibility. All experiments were carried out on a well-controlled laboratory drop-tube furnace (DTF). A high-iron bituminous coal (Illinois No. 6 coal) was burnt in simulated air (21% O_2/79% N_2) and oxy-fuel (O_2/CO_2) environments. Three O_2 levels, i.e., 21, 27, and 32%, were chosen for the oxy-fuel cases, so that the influence of the inlet O_2 level could be investigated.

2. EXPERIMENTAL SECTION

2.1. Fuel Properties. A U.S. high-iron bituminous coal (Illinois No. 6), as used in the previous study,[15] was selected for this work. The proximate and ultimate analysis data and the ash composition data (reported on an ashed sample weight basis after stage ashing in air overnight at 750 °C) are presented in Table 1. This bituminous coal is characterized by high contents of iron (as Fe_2O_3, 14.57% on an ash weight basis) and sulfur (3.98% on a coal weight basis). They may be present mainly as pyrite in the coal. SiO_2 and Al_2O_3 account for about 67% of the ash weight. However, the content of SiO_2 is much higher than that of Al_2O_3, indicating the presence of a significant fraction of quartz.

2.2. Ash Sample Preparation. All bulk ash samples were generated at 1300 °C on a laboratory DTF. Oxy-fuel combustion tests at three O_2 levels (i.e., 21, 27, and 32%) were carried out. For comparison, the coal was also burnt in air, which was simulated by a mixture of 21% O_2/79% N_2. These combustion conditions were defined as follows: (1) AIR, 21 vol % O_2/79 vol % N_2; (2) OXY21, 21 vol % O_2/79 vol % CO_2; (3) OXY27, 27 vol % O_2/73 vol % CO_2; and (4) OXY32, 32 vol % O_2/68 vol % CO_2.

The DTF, as shown in Figure 1, consists of a coal feeding system, high-temperature furnace, and a sampling system. Most of the facility

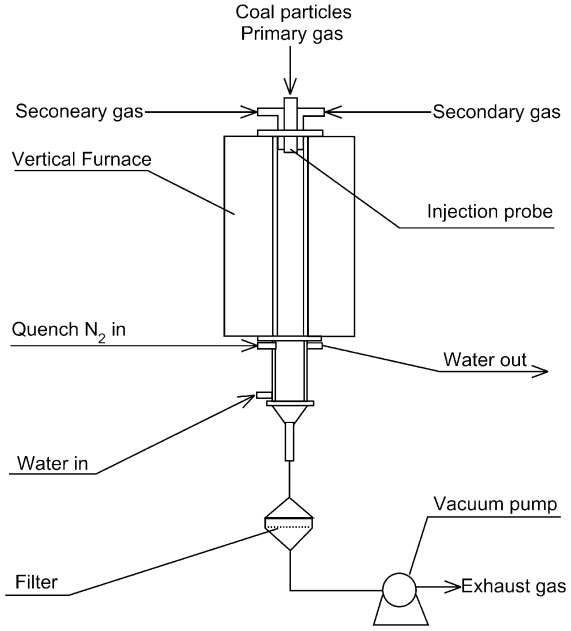

Figure 1. Schematic graph of the experimental facility.

were introduced elsewhere.[16,17] A Sankyo Piotech Micro Feeder (model MFEV-10) was used to push the coal particles into the primary gas stream, which entrained the coal particles into the heated zone of the furnace through a water-cooled injector. The secondary oxidant gas was provided for complete burnout. The furnace has a length of 2 m and an inner diameter of 56 mm. It is electrically heated, and temperature controllers maintain the temperature of the hot zone of the furnace at a constant temperature of 1300 °C for all tests. The coal feeding rate is adjustable, and a value of about 0.3 g/min was selected in this study. For all tests, the flow rate of the oxidant gas stream was maintained at about 6 L/min, providing far excess oxygen to achieve complete combustion. The exit oxygen concentration for different conditions is as follows: 13.2% for AIR and OXY21, 19.1% for OXY27, and 23.9% for OXY32. Loss-on-ignition tests of the ash samples generated under the above combustion conditions showed that carbon-in-ash was always less than 1%, implying that the coal was combusted nearly completely. Under the tested conditions, the particle

dx.doi.org/10.1021/ef201786v | Energy Fuels 2012, 26, 3150−3155

residence time in the DTF was estimated to be around 1.5 s. A water-cooled jacket with pure nitrogen injected was connected to the outlet of the furnace and was used to quench the combustion products. All of the ash particles in the flue gas were collected by glass fiber filters for further analysis.

2.3. Sample Analysis. The chemical composition of the coal ash samples was characterized by an Eagle III micro-X-ray fluorescence (XRF) elemental analyzer (EDAX, Inc.). The considered elements include Na, Mg, Al, Si, P, S, K, Ca, Ti, and Fe. The results are reported in weight percent of their standard oxides. The iron-containing species in the coal and coal ashes were identified by ^{57}Fe Mössbauer spectroscopy (MS) at room temperature. Mössbauer spectra were recorded in transmission mode on a classical constant acceleration electromechanical spectrometer using a ^{57}Co/Pb source. The spectrum of a standard α-Fe foil was used to calibrate the velocity scale and the origin of the isomer shift (IS). The obtained spectra were approximated by the Lorentzian profile function using a standard least-squares procedure. Important parameters, such as IS, quadrupole splitting (QS), and magnetic hyperfine field (MHF), were determined, so that iron-containing phases could be identified. Ash fusion temperatures were obtained through ash fusibility tests on the Digital Imaging Coal Ash Fusibility System (CAF) produced by Carbolite.

3. RESULTS AND DISCUSSION

3.1. XRF Results. The oxide composition (the weight percentages of the ash elements in their oxide forms) of the bulk ashes generated under different combustion conditions is compared in Figure 2. It is evident that the relative proportions

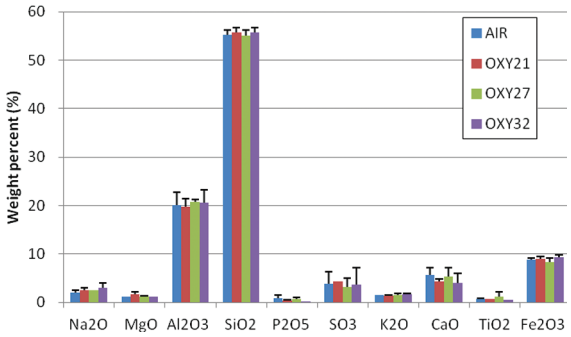

Figure 2. XRF results of ash composition.

of iron oxide (as Fe_2O_3) and other oxides do not differ much between air- and oxy-firing cases. A similar result was obtained when the same coal was burnt in air and mixtures of O_2 and CO_2 on a 100 kW down-fired combustor.[15] It seems to indicate that switching from air-firing to oxy-firing has insignificant effects on ash composition. Nevertheless, some pilot-scale studies reported slightly higher sulfur content in the oxy-fired ash than in the air-fired ash.[18] This was attributed to enhanced ash sulfation because of the higher SO_2/SO_3 concentrations in oxy-firing. It must be emphasized here that bulk analysis techniques, such as XRF and energy-dispersive X-ray spectroscopy (EDS), as used in this work and other studies,[15] actually only provide information on elements rather than their species, although the results are routinely reported in weight percent of their standard oxides. In this regard, similar ash oxide composition based on bulk analysis techniques does not necessarily mean similar species composition, which is more important in determining ash fusibility and its potential deposition propensity. This is evidenced by the fact that XRF results (Figure 2) show a similar content of iron (as Fe_2O_3) in the ash samples from different cases, while Mössbauer spectroscopic analysis shows apparent differences in the contents of iron species, as discussed below. It indicates that speciation analysis is also required for thorough ash characterization.

3.2. Mössbauer Spectroscopic Analysis Results. Data on iron speciation in the coal and its combustion products are summarized in Table 2. As expected, pyrite is the most

Table 2. Mössbauer Spectroscopic Analysis Results

	IS	QS	MHF (kOe)	assignment	Fe (%)
	0.33	0.61		pyrite	64.9
coal	1.27	2.68		Fe−clay	29.5
	0.38	1.17		jarosite	5.6
	0.37	−0.19	511	hematite	28.7
	0.24	1.28		Fe^{3+}−glass	16.1
AIR ash	0.3	0	491	magnetite A	27.4
	0.61	0	455	magnetite B	22
	0.92	1.84		Fe^{2+}−glass	5.8
	0.37	−0.2	508	hematite	32.9
	0.23	1.27		Fe^{3+}−glass	15.7
OXY21 ash	0.31	0	488	magnetite A	27.9
	0.59	0	451	magnetite B	18.3
	0.92	1.8		Fe^{2+}−glass	5.2
	0.36	−0.2	512	hematite	36.9
	0.21	1.32		Fe^{3+}−glass	15
OXY27 ash	0.31	0	491	magnetite A	23.3
	0.62	0	450	magnetite B	19
	0.91	1.73		Fe^{2+}−glass	5.8
	0.36	−0.2	512	hematite	39.1
	0.22	1.3		Fe^{3+}−glass	14.1
OXY32 ash	0.3	0	491	magnetite A	17.2
	0.62	0	450	magnetite B	22.5
	0.92	1.79		Fe^{2+}−glass	7.1

abundant iron-containing mineral (64.9% Fe on a molar basis, with the same basis below) in the coal sample, which is followed by Fe−clay minerals (29.5%). In addition to these commonly observed species, an unusual iron species, namely, jarosite, was also detected. However, it only accounts for a relatively much smaller fraction of 5.6%. Jarosite was believed to be an oxidation product of pyrite, with a general formula of $XFe_3(OH)_6(SO_4)_2$, where X could be H^+, K^+, Na^+, or NH_4^+.[19,20] The oxidation reactions might occur during weathering, storage, and/or transportation of the coal.

The iron species identified in all of the ashes are the same, including hematite (α-Fe_2O_3), magnetite (Fe_3O_4), and Fe−glass phases. Two forms of magnetite with different structures were detected, i.e., magnetite A (tetrahedral) and magnetite B (octahedral). Different Mössbauer parameters indicated two kinds of Fe−glass phases, which were assigned to Fe^{3+}−glass and Fe^{2+}−glass, respectively. The data in Table 2 show that, in the present study, varying combustion conditions does not affect the types of iron species in ashes; however, it does have evident effects on their relative proportions (as detailed below). These results suggest that switching from air- to oxy-firing and increasing the inlet O_2 level do not affect iron transformation pathways but do affect the relative percentages of iron combustion products. Taking the XRF results (Figure 2) into consideration, it is obvious that ash characterization solely by bulk analysis is not enough, and speciation analysis is a very important supplement in elucidating ash-related problems, as mentioned above.

dx.doi.org/10.1021/ef201786v | Energy Fuels 2012, 26, 3150−3155

As shown in Table 2, the combustion condition has apparent effects on the amount of iron species in the ash, suggesting differences in iron transformation. The Mössbauer analysis data on hematite, magnetite, and Fe−glass phases are compared in Figure 3. It is clear that, for all conditions tested, magnetite is

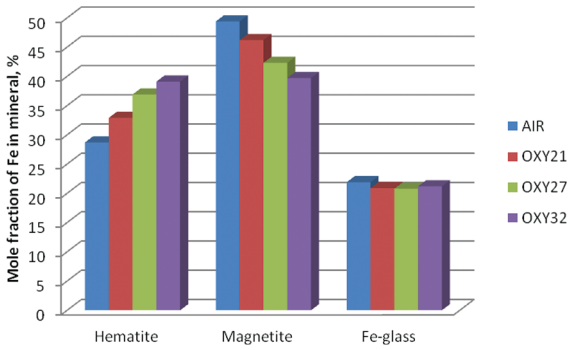

Figure 3. Comparison of iron-containing minerals in coal ashes.

the dominant iron-containing product, followed by hematite and Fe−glass phases. The important result is that oxy-firing always results in more hematite but less magnetite than air-firing. In contrast, the contents of Fe−glass phases are similar in air-fired ash and oxy-fired ashes. Sheng et al. also investigated iron transformation during coal combustion in both O_2/N_2 and O_2/CO_2 with Mössbauer analysis.[13] In contrast, they found that O_2/CO_2 combustion resulted in more iron glass silicates and less iron oxides compared to O_2/N_2 combustion at the same inlet O_2 concentration. This was attributed to the slow transformations of included pyrite and siderite to oxides because of the lower char combustion temperatures and the high CO concentration within the particles, which favored the transformation of the iron minerals to iron glass phases. The inconsistency between this work and the work by Sheng et al.[13] can be explained by assuming that pyrite in the Illinois No. 6 coal is mainly present as excluded minerals. Because the excluded pyrite particles tend to evolve independently into iron oxides during combustion, they would have very few opportunities to interact with silicate minerals within the coal particle. Consequently, the amount of iron in glass phases, which are derived mainly from Fe-containing clay minerals, would be little affected. This assumption is, however, consistent with Figure 3, which shows that the amount of iron in glass phases remains almost unchanged for all combustion cases. It suggests that the assumption that pyrite in the coal tested is mostly excluded in nature is reasonable.

The only difference between AIR and OXY21 cases is the replacement of N_2 with CO_2. Therefore, the differences in iron combustion products from both cases are attributed to the effects of CO_2. According to Bhargava et al.,[11] heating of pyrite in N_2 mainly resulted in pyrrhotite, while heating of pyrite in CO_2 led to the formation of magnetite and hematite. It was attributed to the dissociation of CO_2 into CO and O_2, which favors the oxidation of pyrite to iron oxides. On the other hand, replacing N_2 in air with CO_2 will result in lower particle temperatures because of the higher heat capacity of CO_2.[1] Lower combustion temperatures were reported to favor the oxidation of pyrite to hematite.[5] These findings suggest that, in comparison to AIR, OXY21 will favor the formation of hematite because of the lower temperature and, however, elevated O_2 concentration because of the dissociation of CO_2. Consequently, a larger fraction of hematite and a smaller fraction of magnetite are expected to form for OXY21, consistent with Figure 3.

For the oxy-firing cases (i.e., OXY21, OXY27, and OXY32), with increasing the inlet O_2 level from 21 to 32%, the content of hematite in the ash increases, while the content of magnetite decreases (Figure 3). Increasing the inlet O_2 level is actually accompanied by decreasing the CO_2 level, which is expected to lead to less O_2 released from CO_2 decomposition. However, direct thermal decomposition of CO_2 under conditions tested (1300 °C and 1 atm) is limited, and a very low dissociation (<1%) is expected.[21] Therefore, the elevated inlet O_2 level is believed primarily to account for the higher content of hematite in the ash.

Another interesting result is that the mole fraction of iron as Fe−glass in coal ashes (20.8−21.9%) is generally lower than that of iron as Fe−clays in the raw coal (29.5%). It implies that about 8% Fe in Fe−clays is transformed to magnetite and/or hematite after combustion. The transformation of iron in glass melt to magnetite and/or hematite might occur when the glass became saturated in the iron component. For example, it was reported that magnetite crystallized out of the melt once the melt oxide content exceeded 85%.[22] Figure 3 shows that the combustion condition appears to have an insignificant influence on the production of Fe−glass phases. This indicates that the crystallization of magnetite/hematite from glass melt is little dependent upon combustion conditions. It is most likely related to coal mineralogy.

3.3. Ash Fusibility Test (AFT) Results. The AFT is usually used to determine the temperatures at which the various stages of ash softening and melting take place. It is the most widely accepted means of assessing the deposition characteristics of the coal. Three characteristic temperatures are often determined by the AFT, i.e., the deformation temperature (DT), the softening temperature (ST), and the flow temperature (FT).[23] DT is the temperature at which the tip of the standard ash cone begins to round. ST is taken to be when the height of the cone equals the width of the cone, while FT is when the cone height is about 1.5 mm. The characterization of coal ash for its tendency to slag and foul is closely related to the three ash fusion temperatures. Ash fusion temperatures are highly dependent upon its chemical composition.[24,25] On the basis of the assumption that similar composition resulted in similar ash fusion temperatures, a number of studies tried to predict ash fusion temperatures with bulk ash analysis data.[26−28] However, as discussed in the previous section, bulk analysis cannot identify specific mineral species, which can play important roles in determining ash fusion characteristics.

As shown in Figure 2, the XRF data on the air- and oxy-fired ashes indicate similar oxide composition. Contrary to the expectation, appreciable differences in the ash fusion temperatures (especially DT), as compared in Figure 4, are observed between different cases. Generally, all of the ash fusion temperatures increase in the order AIR < OXY21 < OXY27 < OXY32. This result indicates that the ashes generated in oxy-firing have higher ash fusion temperatures than the ashes generated in air-firing. In addition, for all oxy-firing cases (OXY21, OXY27, and OXY32), the ash fusion temperatures increase with an increasing O_2 level in the oxidant stream. Apparently, the dissimilarity in ash fusion temperatures between different combustion cases cannot be explained by the bulk analysis data. As shown in Table 2 and Figure 3, the contents of iron species in the ash vary with combustion

dx.doi.org/10.1021/ef201786v | Energy Fuels 2012, 26, 3150−3155

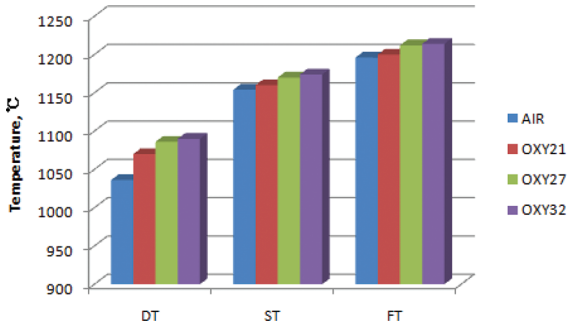

Figure 4. Comparison of ash fusion temperatures.

conditions. Figure 5 depicts the variations of ash fusion temperatures with the content of hematite. The data are also

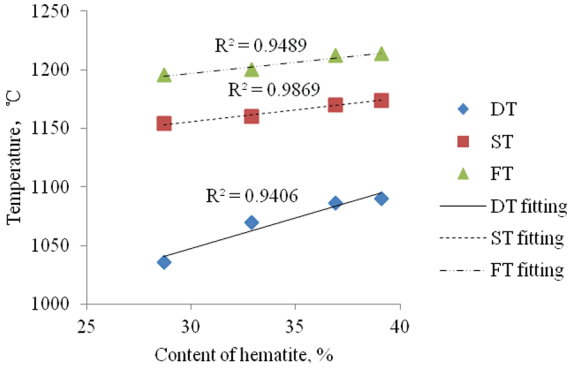

Figure 5. Correlation of ash fusion temperatures with the hematite content.

fitted by straight lines, and a clear positive correlation is observed. It appears that hematite may play an important role in determining ash fusion temperatures, because it has a very high melting point of 1565 °C. Nevertheless, future work is required to elucidate in depth the effects of oxy-firing on ash fusion behaviors.

In the previous study, the Illinois No. 6 coal was also burnt under air-firing (AIR) and two oxy-firing conditions (OXY27 and OXY32).[15] It was found that the deposition tendency (defined as the mass of the ash collected on the deposition probe in an equal time period) of the oxy-fired ashes was higher than that of the air-fired ash and increased with an increasing inlet O_2 level. However, the content of iron (as Fe_2O_3) in the oxy-fired deposits was lower than that in the air-fired deposit and decreased with an increasing inlet O_2 level. Although aerodynamic changes could be an important reason, the changes in the formation of iron species might be another reason. As shown by the present work, in comparison to the AIR case, the OXY27 and OXY32 cases favor the formation of hematite. In addition, the content of hematite increases with an increasing inlet O_2 level. Because hematite has a high melting point, the more hematite is formed, the less hematite-containing particles are expected to deposit onto the deposition coupon, resulting in a lower content of iron in the deposit. This is consistent with the observations obtained from the 100 kW down-fired combustor.[15]

4. CONCLUSION

A high-iron bituminous coal was burnt in both O_2/N_2 and O_2/CO_2 in a laboratory DTF. The effects of changing from O_2/N_2 combustion to O_2/CO_2 combustion and the effects of varying the O_2 level in O_2/CO_2 combustion on iron transformation and ash fusibility were investigated. The following results are obtained: (1) Switching from O_2/N_2 combustion to O_2/CO_2 combustion has insignificant effects on the oxide composition of the coal ash. Similar results are observed when varying the O_2 level in O_2/CO_2 combustion. (2) The identified iron-containing species in each coal ash are the same, including hematite, magnetite, and Fe–glass phases. The contents of hematite and magnetite are significantly affected by changing combustion conditions, while the content of Fe–glass phases is much less affected. (3) Changing from O_2/N_2 combustion to O_2/CO_2 combustion increases the formation of hematite but decreases the formation of magnetite. Increasing the O_2 level in O_2/CO_2 combustion favors the formation of hematite. (4) An appreciable fraction of hematite/magnetite seems to crystallize out of the molten glass phases during combustion. The fraction is not significantly affected by changing combustion conditions. (5) Changing from O_2/N_2 combustion to O_2/CO_2 combustion or increasing the O_2 level in O_2/CO_2 combustion increases ash fusion temperatures. A positive correlation between the hematite content and the ash fusion temperatures is observed.

AUTHOR INFORMATION

Corresponding Author

*Telephone: 86-27-87545526. Fax: 86-27-87545526. E-mail: yudunxi@hust.edu.cn.

ACKNOWLEDGMENTS

This work is supported by the National Natural Science Foundation of China under Awards 51076051 and 51021065, the National Key Scientific Instruments and Equipment Funding (Grant No. 2011YQ120039), and the Specialized Research Fund for the Doctoral Program of Higher Education (Grant No. 20110142110075). The assistance with Mössbauer spectroscopic analysis and data interpretation from Dr. Jun Lin at Shanghai Institute of Applied Physics, Chinese Academy of Sciences, is highly appreciated.

REFERENCES

(1) Wall, T.; Liu, Y.; Spero, C.; Elliott, L.; Khare, S.; Rathnam, R.; Zeenathal, F.; Moghtaderi, B.; Buhre, B.; Sheng, C.; Gupta, R.; Yamada, T.; Makino, K.; Yu, J. *Chem. Eng. Res. Des.* **2009**, *87* (8), 1003–1016.

(2) Russell, N. V.; Wigley, F.; Williamson, J. *Fuel* **2002**, *81* (5), 673–681.

(3) Taneja, S. P.; Jones, C. H. W. *Fuel* **1984**, *63* (5), 695–701.

(4) Zeng, T.; Helble, J. J.; Bool, L. E.; Sarofim, A. F. *Fuel* **2009**, *88* (3), 566–572.

(5) Hu, G.; Dam-Johansen, K.; Wedel, S.; Hansen, J. P. *Prog. Energy Combust. Sci.* **2006**, *32* (3), 295–314.

(6) ten Brink, H. M.; Eenkhoorn, S.; Weeda, M. *Fuel Process. Technol.* **1996**, *47* (3), 233–243.

(7) McLennan, A. R.; Bryant, G. W.; Bailey, C. W.; Stanmore, B. R.; Wall, T. F. *Energy Fuels* **2000**, *14* (2), 349–354.

(8) Buhre, B. J. P.; Elliott, L. K.; Sheng, C. D.; Gupta, R. P.; Wall, T. F. *Prog. Energy Combust. Sci.* **2005**, *31* (4), 283–307.

(9) Krishnamoorthy, G.; Veranth, J. M. *Energy Fuels* **2003**, *17* (5), 1367–1371.

(10) Wall, T. F. *Proc. Combust. Inst.* **2007**, *31* (1), 31–47.

(11) Bhargava, S. K.; Garg, A.; Subasinghe, N. D. *Fuel* **2009**, *88* (6), 988–993.

(12) Fegley, B. Jr.; Lodders, K.; Treiman, A. H.; Klingelhöfer, G. *Icarus* **1995**, *115* (1), 159–180.

(13) Sheng, C.; Li, Y. *Fuel* **2008**, *87* (7), 1297–1305.

(14) Sheng, C.; Lin, J.; Li, Y.; Wang, C. *Asia-Pac. J. Chem. Eng.* **2009**, *5* (2), 304−309.
(15) Yu, D.; Morris, W. J.; Erickson, R.; Wendt, J. O. L.; Fry, A.; Senior, C. L. *Int. J. Greenhouse Gas Control* **2011**, *5* (Supplement1), S159−S167.
(16) Yu, D. X.; Xu, M. H.; Yao, H.; Sui, J. C.; Liu, X. W.; Yu, Y.; Cao, Q. *Proc. Combust. Inst.* **2007**, *31* (2), 1921−1928.
(17) Yu, D. X.; Xu, M. H.; Yu, Y.; Liu, X. W. *Energy Fuels* **2005**, *19* (6), 2488−2494.
(18) Stanger, R.; Wall, T. *Prog. Energy Combust. Sci.* **2010**, *37* (1), 69−88.
(19) Creelman, R. A.; Ward, C. R. *Int. J. Coal Geol.* **1996**, *30* (3), 249−269.
(20) Vassilev, S. V.; Vassileva, C. G. *Fuel Process. Technol.* **1996**, *48* (2), 85−106.
(21) Galvez, M. E.; Loutzenhiser, P. G.; Hischier, I.; Steinfeld, A. *Energy Fuels* **2008**, *22* (5), 3544−3550.
(22) Srinivasachar, S.; Helble, J. J.; Boni, A. A. *Prog. Energy Combust. Sci.* **1990**, *16* (4), 281−292.
(23) Wall, T. F.; Creelman, R. A.; Gupta, R. P.; Gupta, S. K.; Coin, C.; Lowe, A. *Prog. Energy Combust. Sci.* **1998**, *24* (4), 345−353.
(24) Qiu, J. R.; Li, F.; Zheng, Y.; Zheng, C. G.; Zhou, H. C. *Fuel* **1999**, *78* (8), 963−969.
(25) Vassilev, S. V.; Kitano, K.; Takeda, S.; Tsurue, T. *Fuel Process. Technol.* **1995**, *45* (1), 27−51.
(26) Seggiani, M. *Fuel* **1999**, *78* (9), 1121−1125.
(27) Vincent, R. G. *Fuel* **1987**, *66* (9), 1230−1239.
(28) Yin, C.; Luo, Z.; Ni, M.; Cen, K. *Fuel* **1998**, *77* (15), 1777−1782.